X-ray spectroscopy of the brightest γ-ray nova ASASSN-18fv

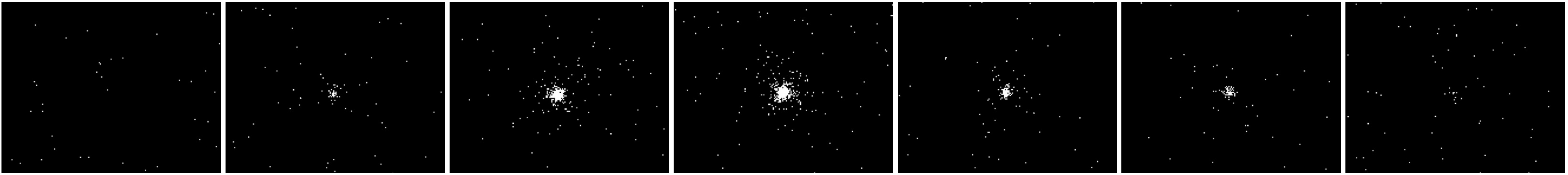

Swift/XRT images of a nova 50 to 400 days post-explosion

Kirill Sokolovsky, Elias Aydi, Laura Chomiuk, Adam Kawash (Michigan State University), Koji Mukai (NASA/GSFC), Raimundo Lopes (Universidade Federal de Sergipe), Thomas Nelson (University of Pittsburgh), Brian D. Metzger, Elad Steinberg (Columbia University)

Classical novae emit X-rays

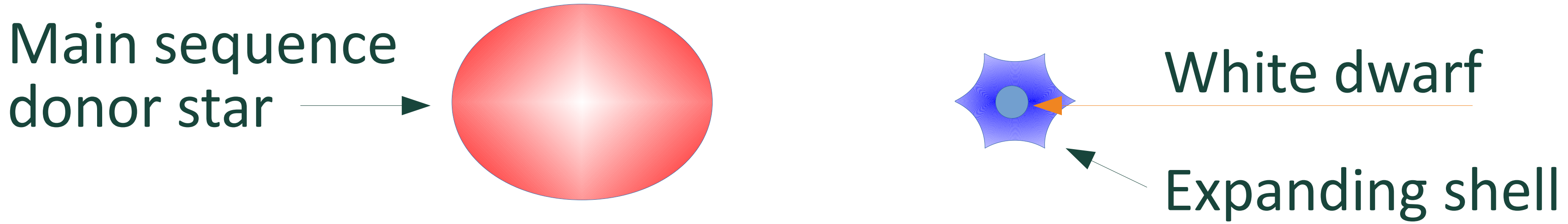

- **X-ray fireball in first hours of explosion** (never observed)
- Shock waves heat plasma and accelerate particles weeks-months after explosion
- Hydrogen-burning white dwarf - "Super-Soft Source"
- When accretion restarts, the gas hitting WD surface gets shocked and heated to X-ray temperatures

Classical novae emit X-rays

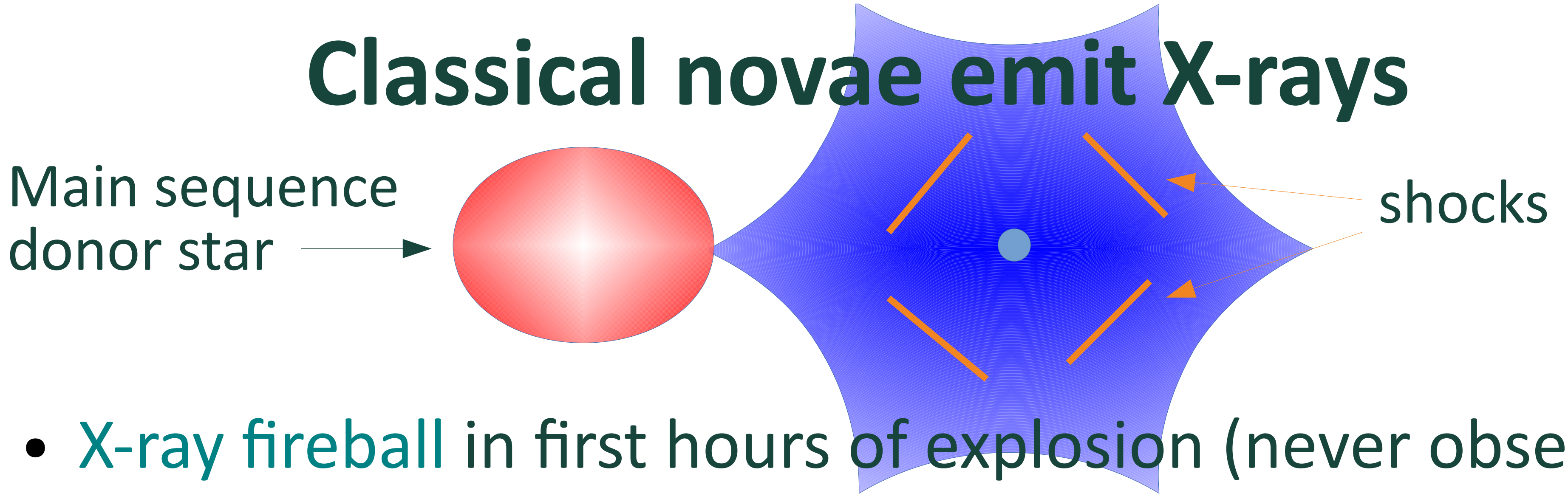

- X-ray fireball in first hours of explosion (never observed)
- **Shock waves heat plasma and accelerate particles weeks-months after explosion**
- Hydrogen-burning white dwarf - “Super-Soft Source”
- When accretion restarts, the gas hitting WD surface gets shocked and heated to X-ray temperatures

Classical novae emit X-rays

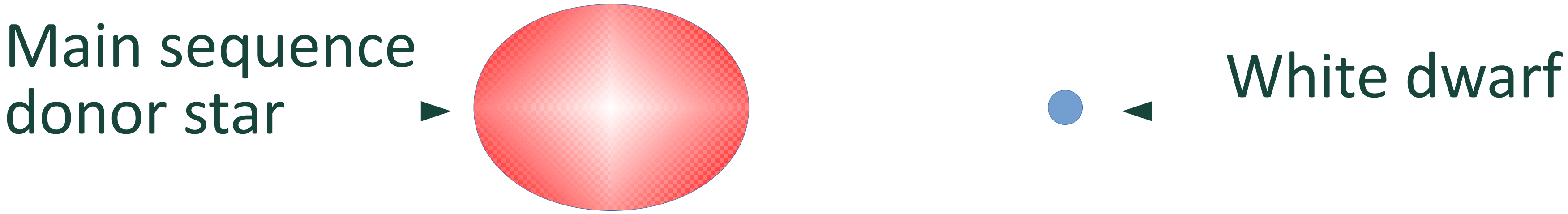

- X-ray fireball in first hours of explosion (never observed)
- Shock waves heat plasma and accelerate particles weeks-months after explosion
- **Hydrogen-burning white dwarf - "Super-Soft Source"**
- When accretion restarts, the gas hitting WD surface gets shocked and heated to X-ray temperatures

Classical novae emit X-rays

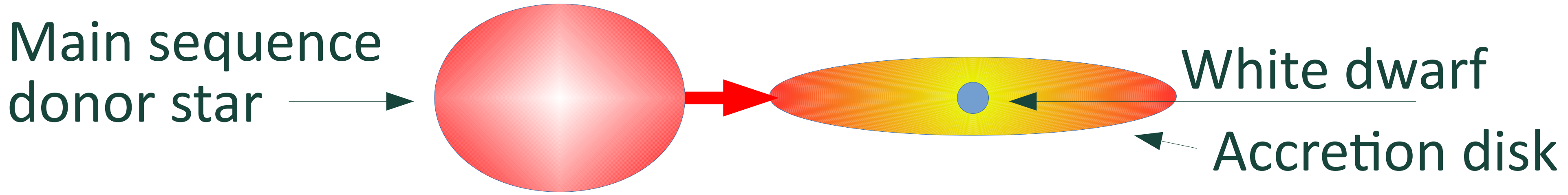

- **X-ray fireball** in first hours of explosion (never observed)
- **Shock waves** heat plasma and accelerate particles weeks-months after explosion
- **Hydrogen-burning white dwarf** - "Super-Soft Source"
- **When accretion restarts, the gas hitting WD surface gets shocked and heated to X-ray temperatures**

X-ray observatories

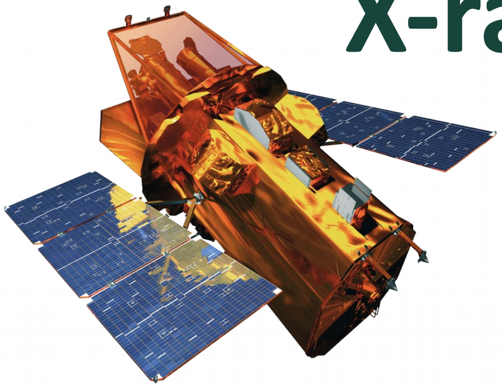

- **Swift** (0.3-10 keV): fast repointing -> can do long-term monitoring

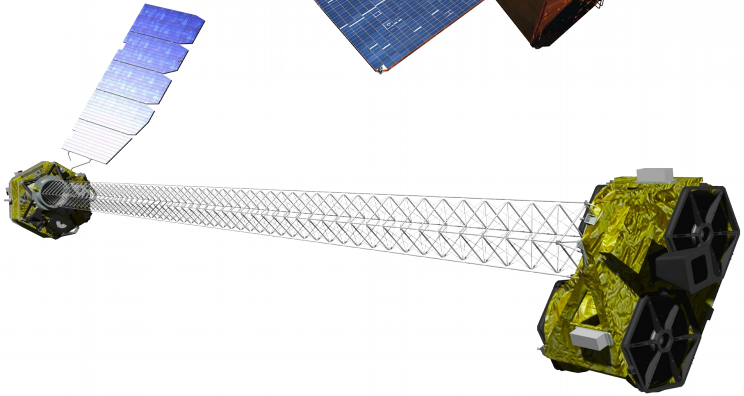

- **NuSTAR** (3-78 keV): exceptional sensitivity to hard X-rays

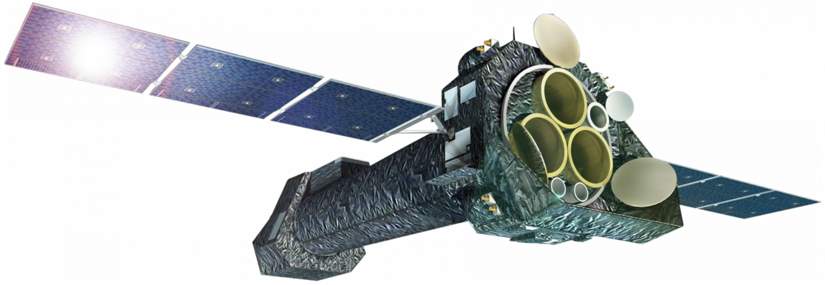

- **XMM-Newton** & **Chandra**: can do high-resolution spectroscopy with X-ray gratings

Nova Cir 2018: Super-Soft Source

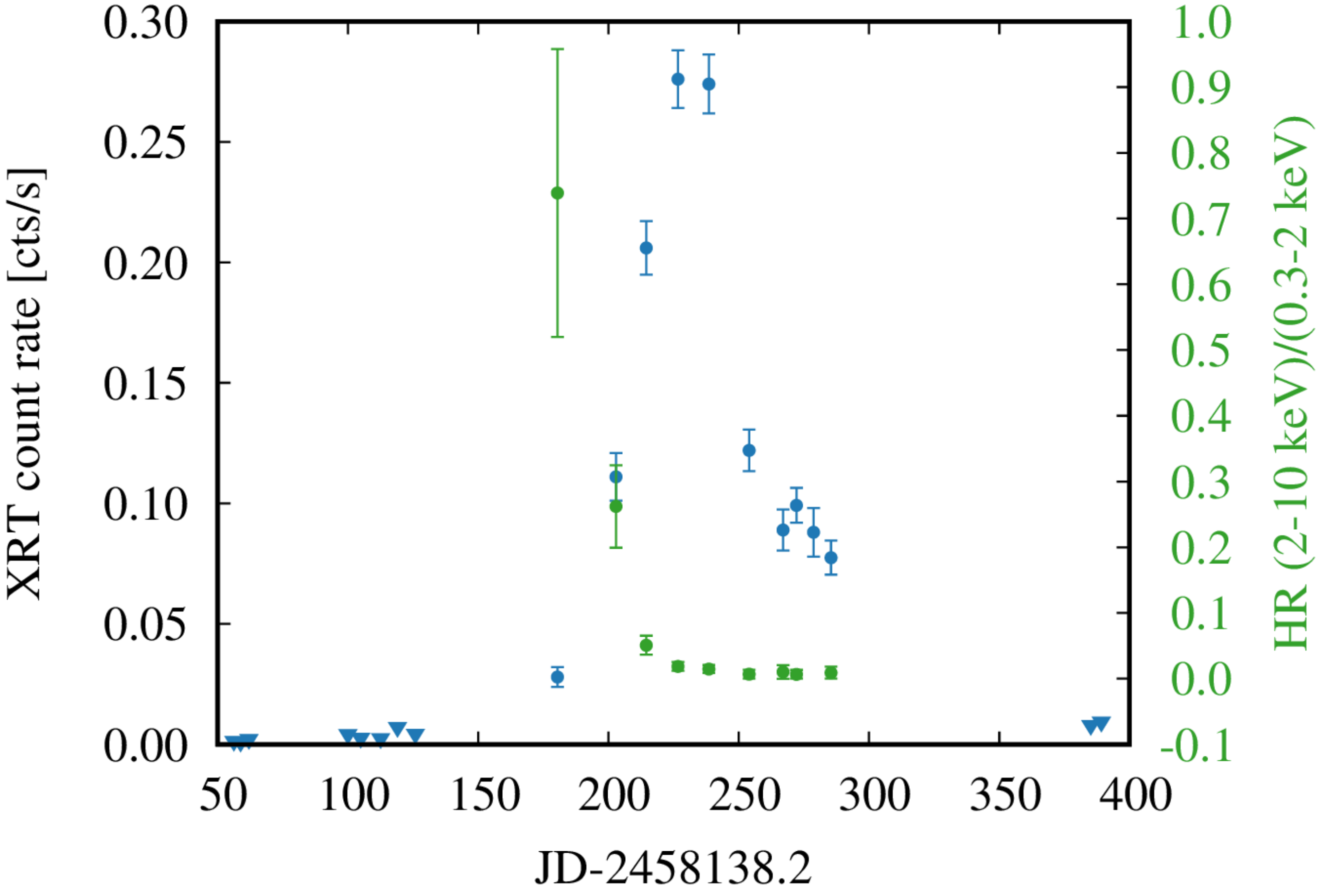

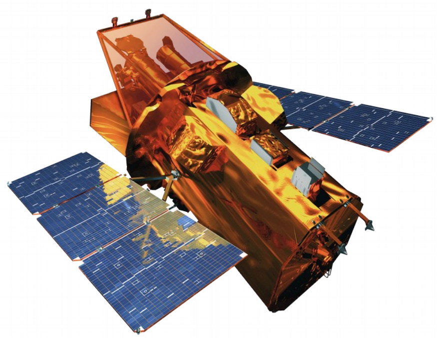

V392 Per: accretion-powered X-rays?

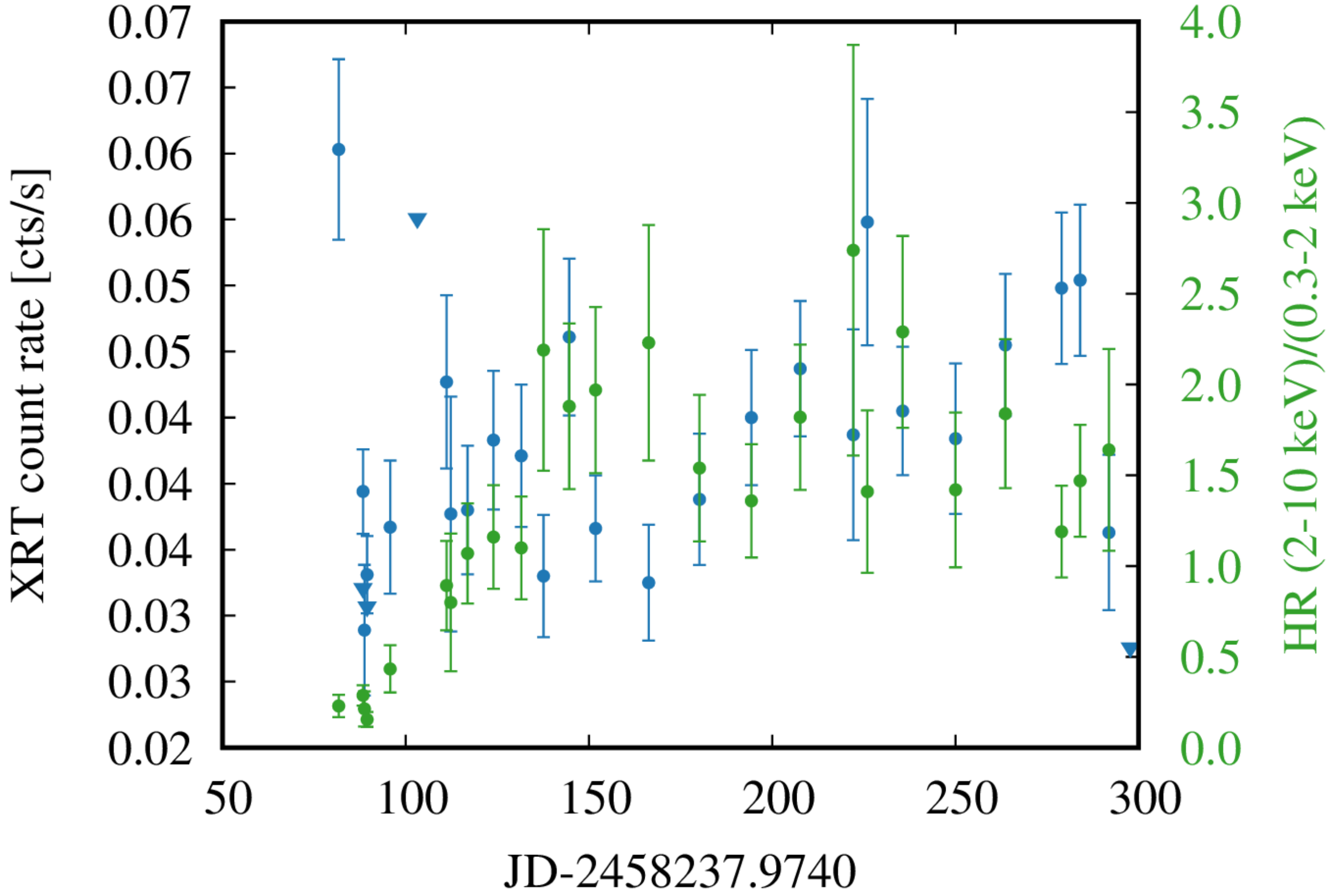

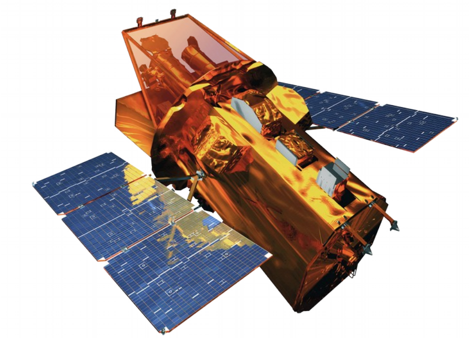

ASASSN-18fv: shocks to Super-Soft

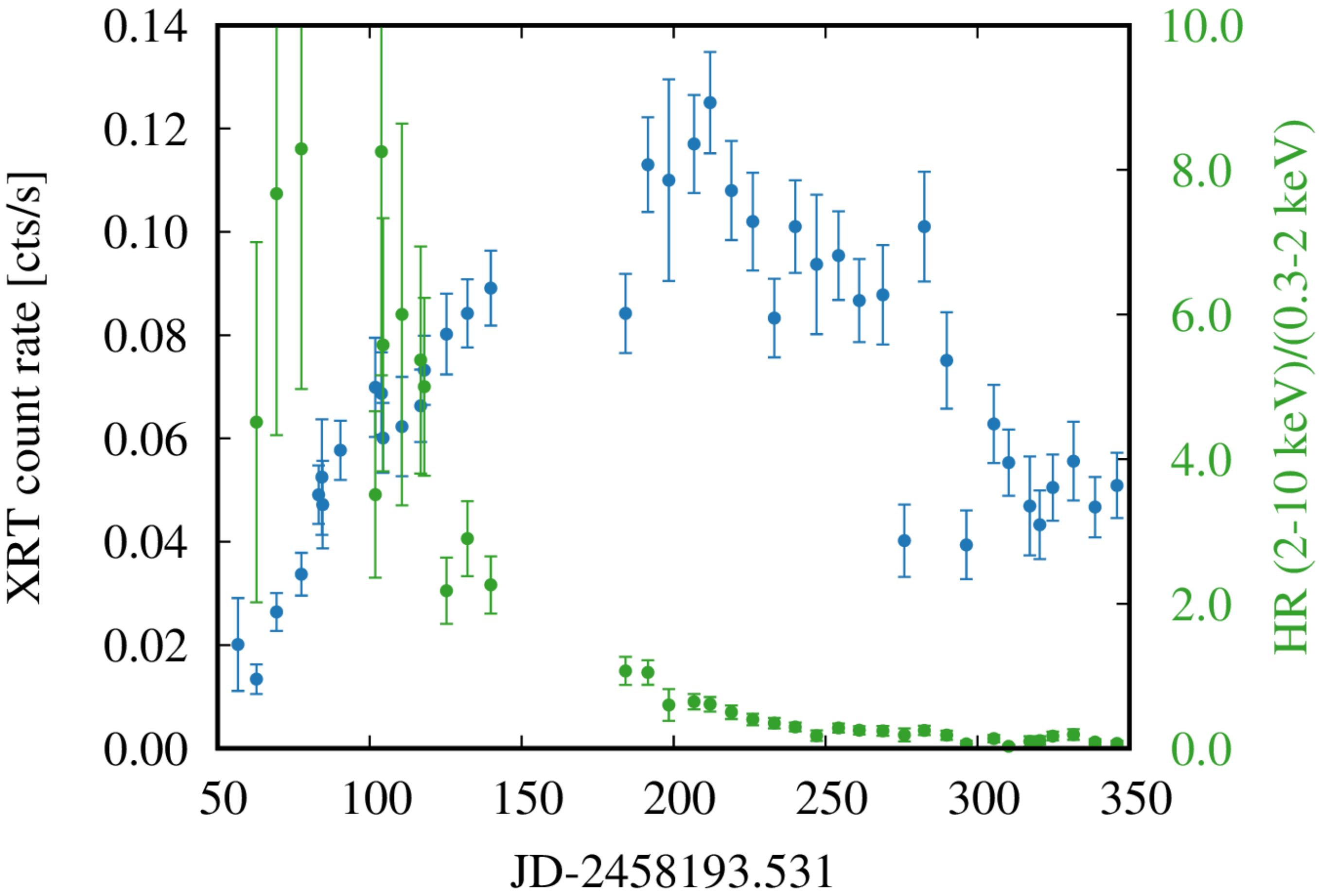

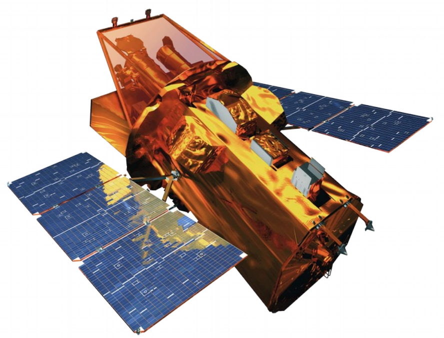

ASASSN-18fv: shocks to Super-Soft

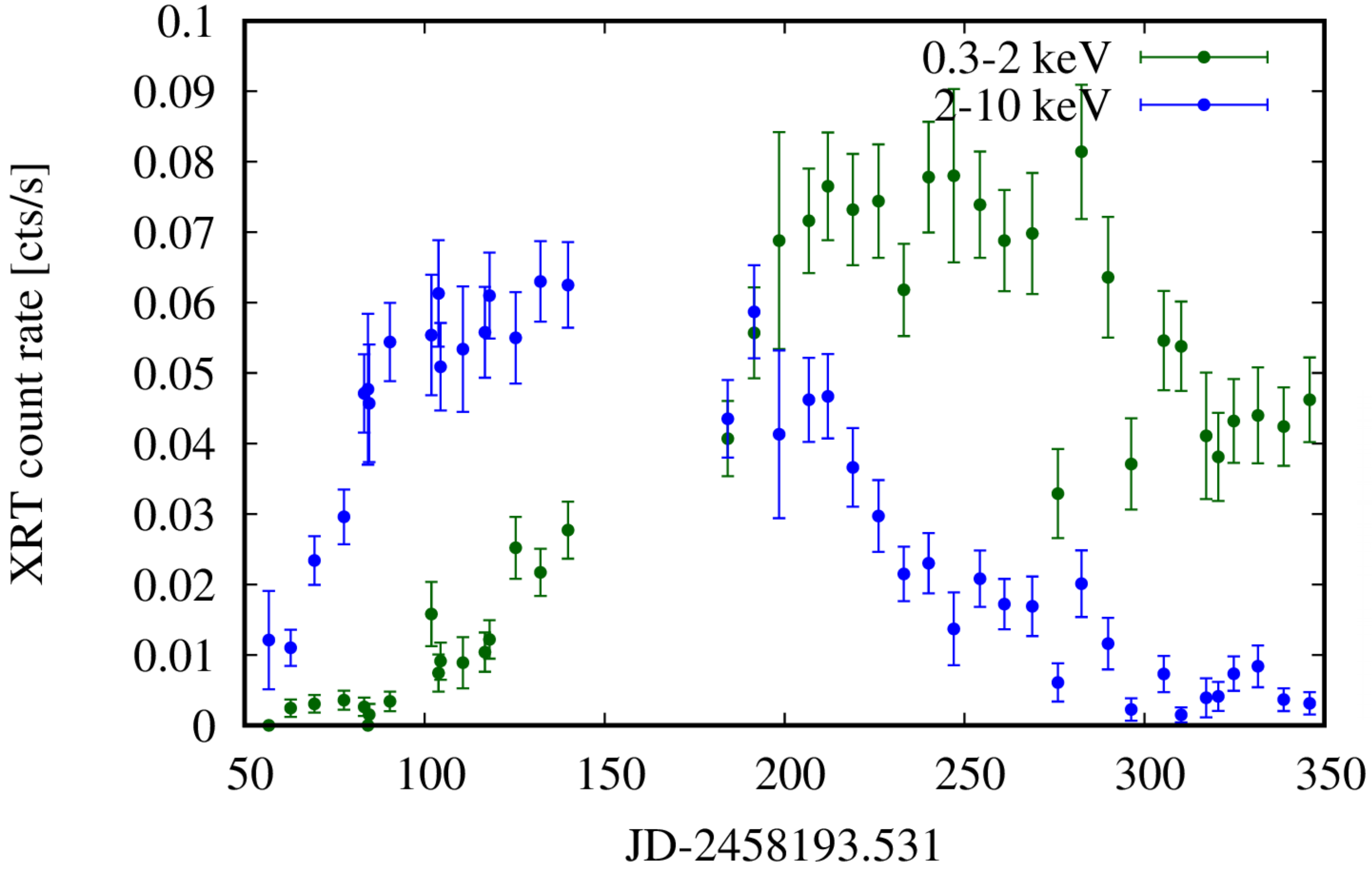

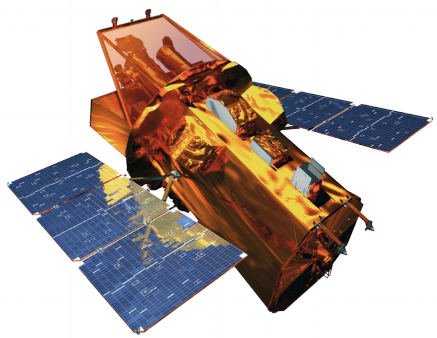

ASASSN-18fv = N Car 2018 = V906 Car

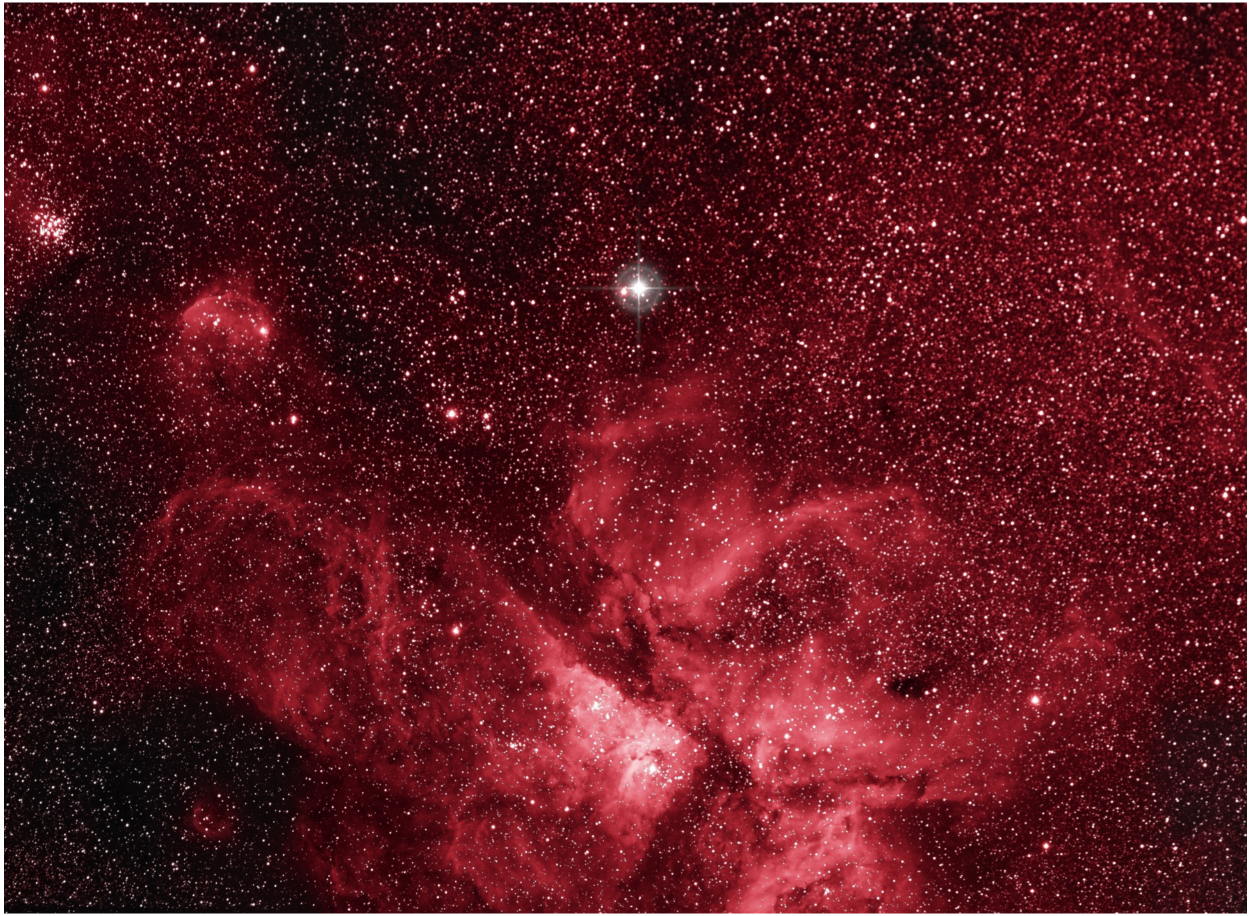

ASASSN-18fv and η Car nebula imaged by Joseph Brimacombe

Discovered 2018-03-20.32 UT by the ASAS-SN survey

ASASSN-18fv = N Car 2018 = V906 Car

ASASSN-18fv and η Car nebula imaged by Joseph Brimacombe

Discovered 2018-03-20.32 UT by the ASAS-SN survey

MW observations of ASASSN-18fv

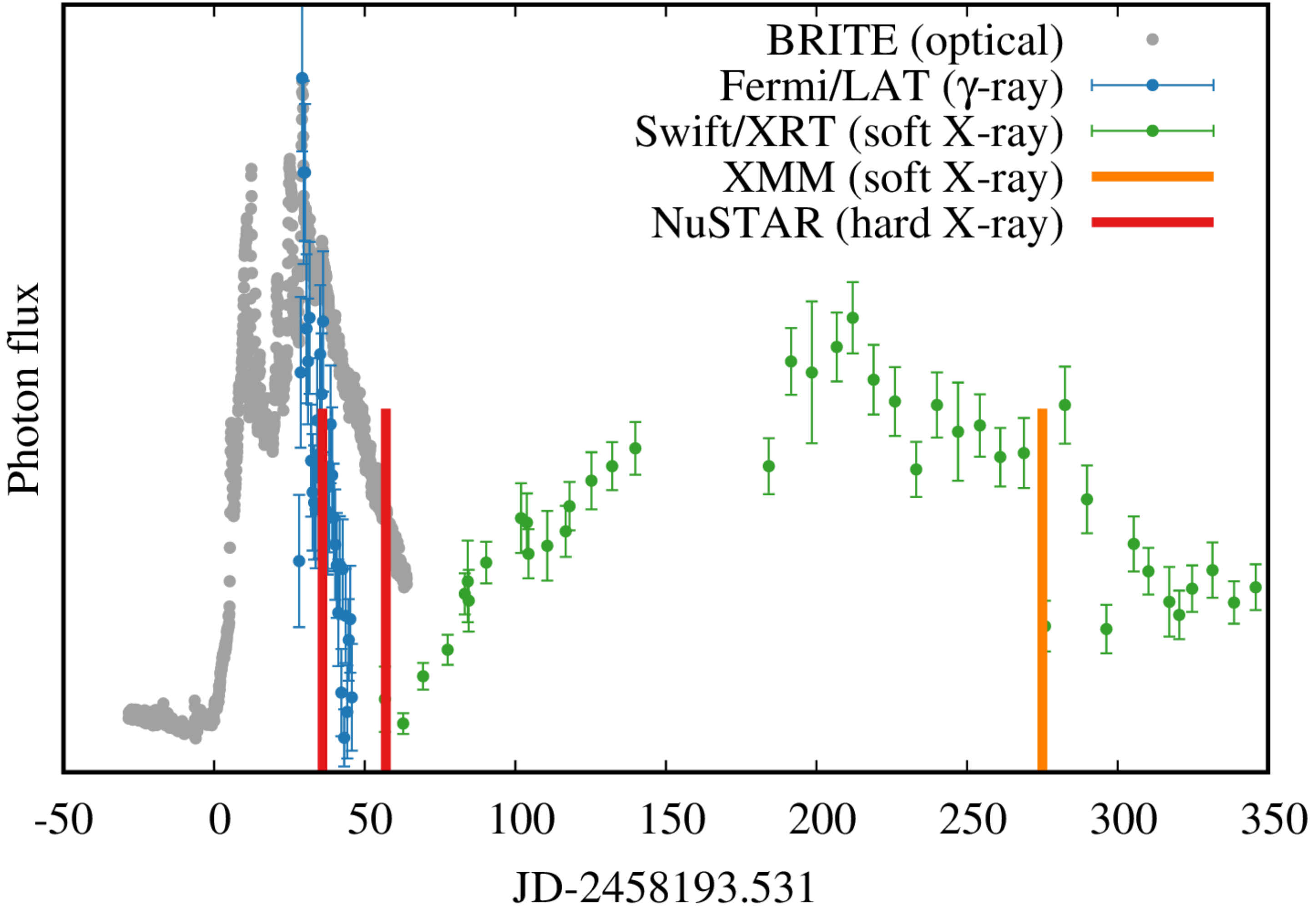

Nova Car 2018: NuSTAR spectra

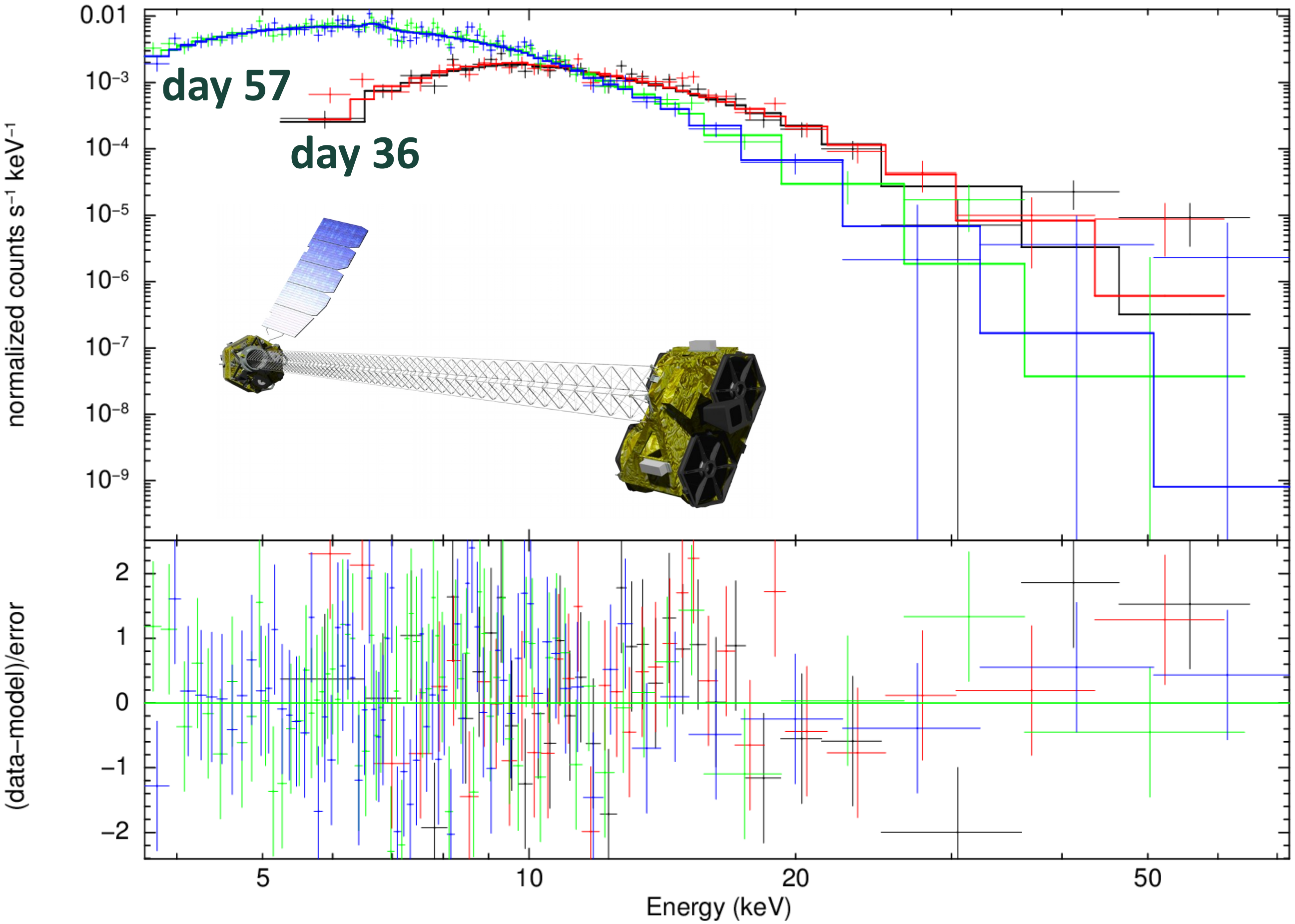

day 36:
kT = 8.6 +-0.9 keV
nHI = 4.3 +-2.3 x10^22 cm^-2
F = 2.7 x10^-12 ergs/s/cm^2

day 57:
kT = 4.4 +-0.2 keV
nHI = 0.6 +-0.3 x10^22 cm^-2
F = 3.5 x10^-12 ergs/s/cm^2

CNO overabundance w.r.t. solar = 210 +-110

no non-thermal emission

NuSTAR observations of novae

Five novae observed so far:

- **V745 Sco** (WD+RG) - detected (Orio et al. 2015)
- **V339 Del** - not detected (Mukai et al. in prep.)
- **V5668 Sgr** - not detected (Mukai et al. in prep.)
- **V5855 Sgr** - detected while still γ-ray bright (Nelson et al. 2019)
- **ASASSN-18fv** - detected while still γ-ray bright

Consistent with thermal emission in all cases

XMM observations of ASASSN-18fv

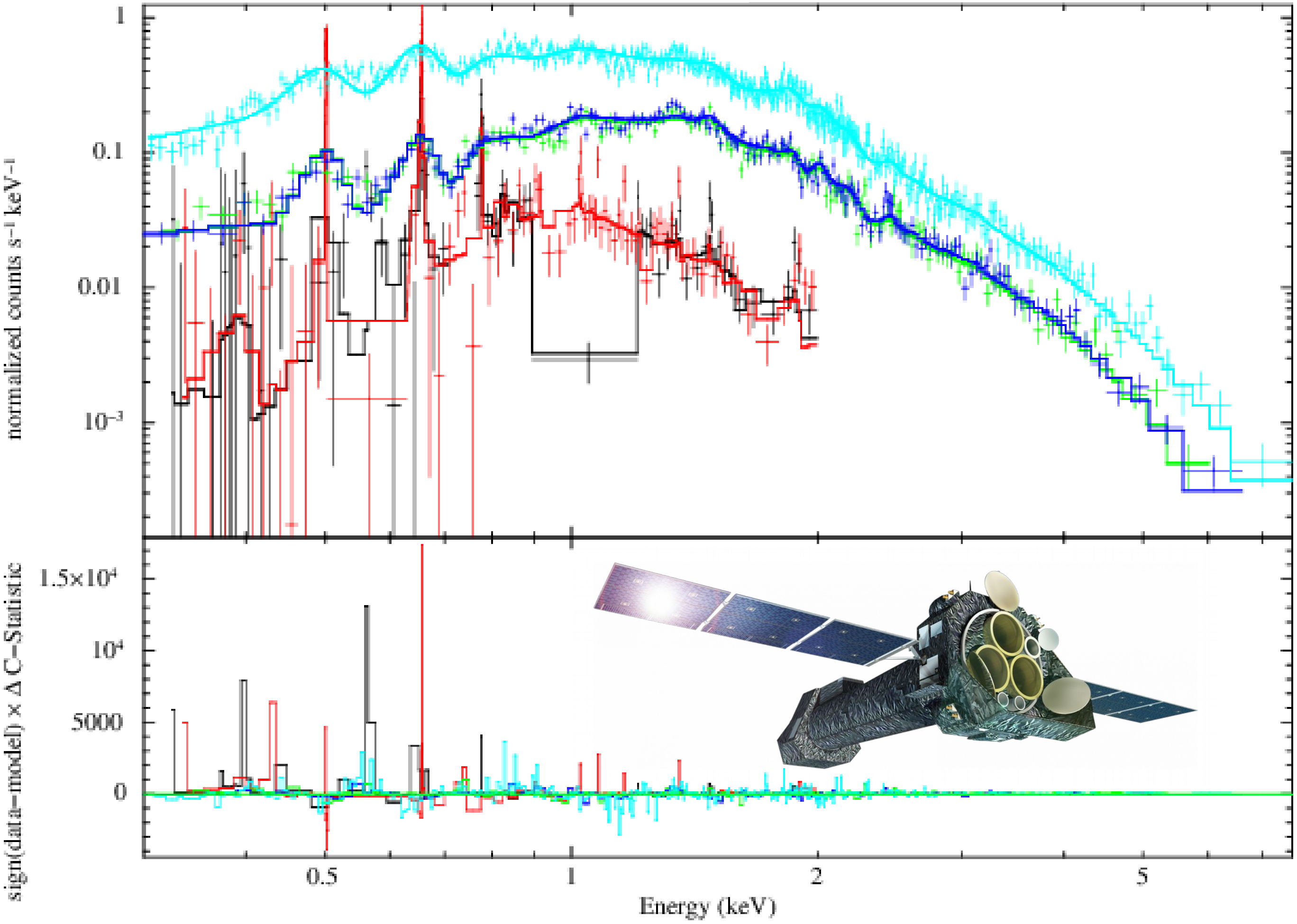

constant*phabs*vphabs*bvapec

	EPIC+RGS
PHABS	
N_H ($\times10^{21}$ cm^{-2})	$2.4^{+0.4}_{-0.3}$
VPHABS	
N_H ($\times10^{21}$ cm^{-2})	$0.12^{+0.03}_{-0.03}$
BVAPEC	
kT (keV)	$1.07^{+0.04}_{-0.01}$
redshift	$-2.9\times10^{-3*}$
velocity (km s^{-1})	$378^{(*)}$
$N/N_\odot$	345^{+93}_{-70}
$O/O_\odot$	29^{+7}_{-5}
$Ne/Ne_\odot$	$2.2^{+0.6}_{-0.5}$
$Mg/Mg_\odot$	$0.6^{+0.2}_{-0.1}$
$Si/Si_\odot$	$1.1^{+0.2}_{-0.2}$
$Fe/Fe_\odot$	<0.1
χ^2_ν	1.15
d.o.f.	1837

XMM observations of ASASSN-18fv

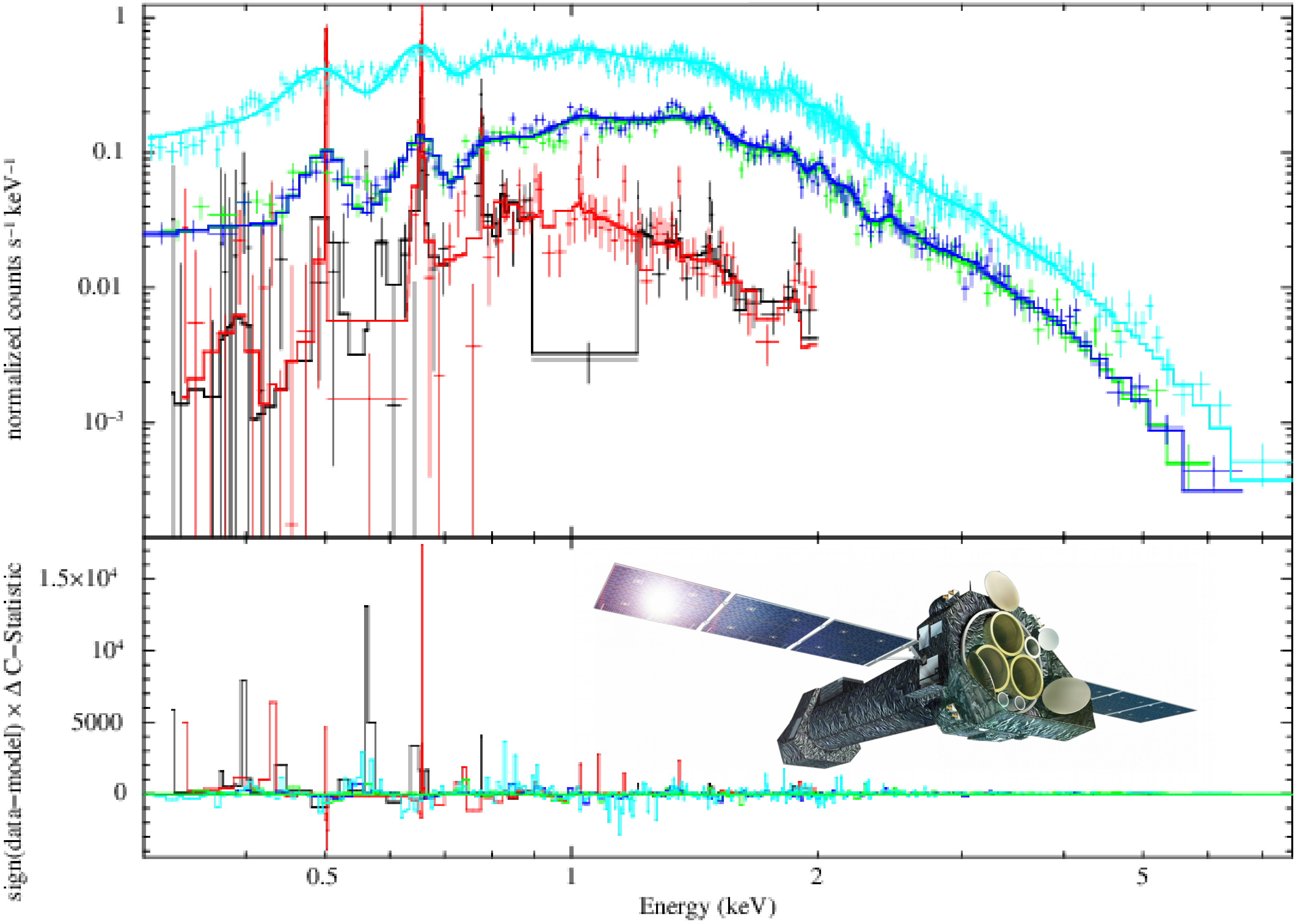

`constant*phabs*vphabs*bvapec`

	EPIC+RGS
PHABS	
N_H ($\times10^{21}$ cm^{-2})	$2.4^{+0.4}_{-0.3}$
VPHABS	
N_H ($\times10^{21}$ cm^{-2})	$0.12^{+0.03}_{-0.03}$
BVAPEC	
kT (keV)	$1.07^{+0.04}_{-0.01}$
redshift	$-2.9\times10^{-3*}$
velocity (km s^{-1})	$378^{(*)}$
N/N$_\odot$	345^{+93}_{-70}
O/O$_\odot$	29^{+7}_{-5}
Ne/Ne$_\odot$	$2.2^{+0.6}_{-0.5}$
Mg/Mg$_\odot$	$0.6^{+0.2}_{-0.1}$
Si/Si$_\odot$	$1.1^{+0.2}_{-0.2}$
Fe/Fe$_\odot$	<0.1
χ^2_ν	1.15
d.o.f.	1837

Outlook

- X-rays provide a **new window on nova physics**
- **Shock energy**, **abundances**, **ejecta mass**, **non-thermal emission**
- Constrains on **particle acceleration** from X-ray/GeV
- **Where**, **when** and **why shocks** are formed?
- Relevant for distant **shock-powered transients**: Type IIn SNe, TDEs, stellar mergers

White paper on shocks by Chomiuk et al. (2019)

NuSTAR observations of ASASSN-18fv

NuSTAR observing log

ObsID	Epoch (days)	Start UT	Stop UT	Exposure FPMA (ks)	Exposure FPMB (ks)	Net count rate FPMA (cts/s)	Net count rate FPMB (cts/s)
80301306002	36.3	2018-04-20 14:46	2018-04-22 02:01	48.8	48.5	0.01582 ± 0.00066	0.01630 ± 0.00067
90401322002	57.2	2018-05-11 16:26	2018-05-12 18:01	47.5	47.4	0.04343 ± 0.00102	0.04184 ± 0.00101

Column designation: Col. 1 – observation identification number; Col. 2 – time since outburst; Col. 3 and 4 – start and stop time of the observation (interrupted by Earth occultations and South Atlantic Anomaly passes); Col. 5 and 6 – total on-source exposure time for FPMA and FPMB, respectively; Col. 7 and 8 – source count rate (background-subtracted) for FPMA and FPMB, respectively.

`constant*vphabs*vapec` model for the two *NuSTAR* observations

Epoch (days)	n_{HI} ($\times 10^{22}\,\mathrm{cm}^{-2}$)	kT (keV)	CNO abundances	C_{FPMB}	Model 3.5-78.0 keV flux $\log_{10}(\mathrm{ergs/cm^2/s})$
		$\chi^2_{\mathrm{red}} = 1.0457$, d.o.f. $= 199$, $p = 0.31$			
36	4.287 ± 2.288	8.59 ± 0.88	209.6 ± 110.4	1.107 ± 0.062	-11.564 ± 0.012
57	0.568 ± 0.288	4.38 ± 0.17		1.006 ± 0.034	-11.454 ± 0.007

	Case 1 EPIC+RGS	Case 2 EPIC+RGS	Case 3 EPIC+RGS	Case 4 RGS	Case 5 RGS
PHABS					
N_H ($\times 10^{21}$ cm^{-2})	$1.8^{+0.3}_{-0.2}$	$1.8^{+0.2}_{-0.2}$	$2.4^{+0.4}_{-0.3}$	$2.1^{+0.5}_{-1.0}$	$2.0^{+2.1}_{-1.0}$
VPHABS					
N_H ($\times 10^{21}$ cm^{-2})	$0.08^{+0.02}_{-0.02}$	$0.13^{+0.03}_{-0.02}$	$0.12^{+0.03}_{-0.03}$	<0.4	<0.4
BVAPEC					
kT (keV)	$1.06^{+0.01}_{-0.01}$	$1.11^{+0.01}_{-0.01}$	$1.07^{+0.04}_{-0.01}$	$0.79^{+0.04}_{-0.10}$	$0.98^{+0.15}_{-0.12}$
redshift	$(-2.9\pm0.1)\times10^{-3}$	$(-2.9\pm0.2)\times10^{-3}$	$-2.9\times10^{-3*}$	$(-3.1\pm0.2)\times10^{-3}$	$-2.9\times10^{-3(*)}$
velocity (km s^{-1})	394 ± 70	378 ± 72	$378^{(*)}$	386^{+72}_{-76}	378^{*}
$N/N_\odot$	728^{+232}_{-150}	403^{+99}_{-73}	345^{+93}_{-70}	230^{+236}_{-81}	212^{+197}_{-87}
$O/O_\odot$	30^{+7}_{-6}	24^{+4}_{-5}	29^{+7}_{-5}	14^{+15}_{-5}	17^{+12}_{-5}
$Ne/Ne_\odot$	$0.7^{+0.6}_{-0.5}$	$2.3^{+0.6}_{-0.5}$	$2.2^{+0.6}_{-0.5}$	$1.1^{+1.3}_{-0.5}$	$1.5^{+1.3}_{-0.7}$
$Mg/Mg_\odot$	$1.0^{+0.2}_{-0.2}$	$0.7^{+0.2}_{-0.1}$	$0.6^{+0.2}_{-0.1}$	$1.0^{+1.0}_{-0.3}$	$0.9^{+0.6}_{-0.3}$
$Si/Si_\odot$	$1.6^{+0.4}_{-0.3}$	$1.2^{+0.2}_{-0.2}$	$1.1^{+0.2}_{-0.2}$	$1.0^{+2.1}_{-0.7}$	$2.0^{+1.3}_{-0.5}$
$Fe/Fe_\odot$	$0.17^{+0.08}_{-0.05}$	<0.1	<0.1	<0.13	<0.04
χ^2_ν	1.25	1.16	1.15	1.01	1.01
d.o.f.	1847	1488	1837	987	977

Notes:

Model CONSTANT*PHABS*VPHABS*BVAPEC in four different cases:

Case 1: in the whole spectral coverage, without Gaussian lines;

Case 2: excluding spectral regions associated with (r,i,f) lines: 0.4-0.45 keV, 0.55-0.6 keV, 0.85-0.95 keV, and 1.3-1.4 keV;

Case 3: in the whole spectral coverage, including Gaussian lines associated with r,i,f lines (Table 3);

Case 4: only RGS, without Gaussian lines;

Case 5: only RGS, with Gaussian lines associated with r,i,f lines (Table 3);

Abundance table: aspl: Asplund M, Grevesse N., Sauval A.J. & Scott P., 2009, ARAA, 47, 481;

Swift obs. of novae

~100 observed,
60% detected,
a few lightcurves

Reviews:
Ness et al. (2007),
Schwarz et al. (2011),
Osborne (2015)

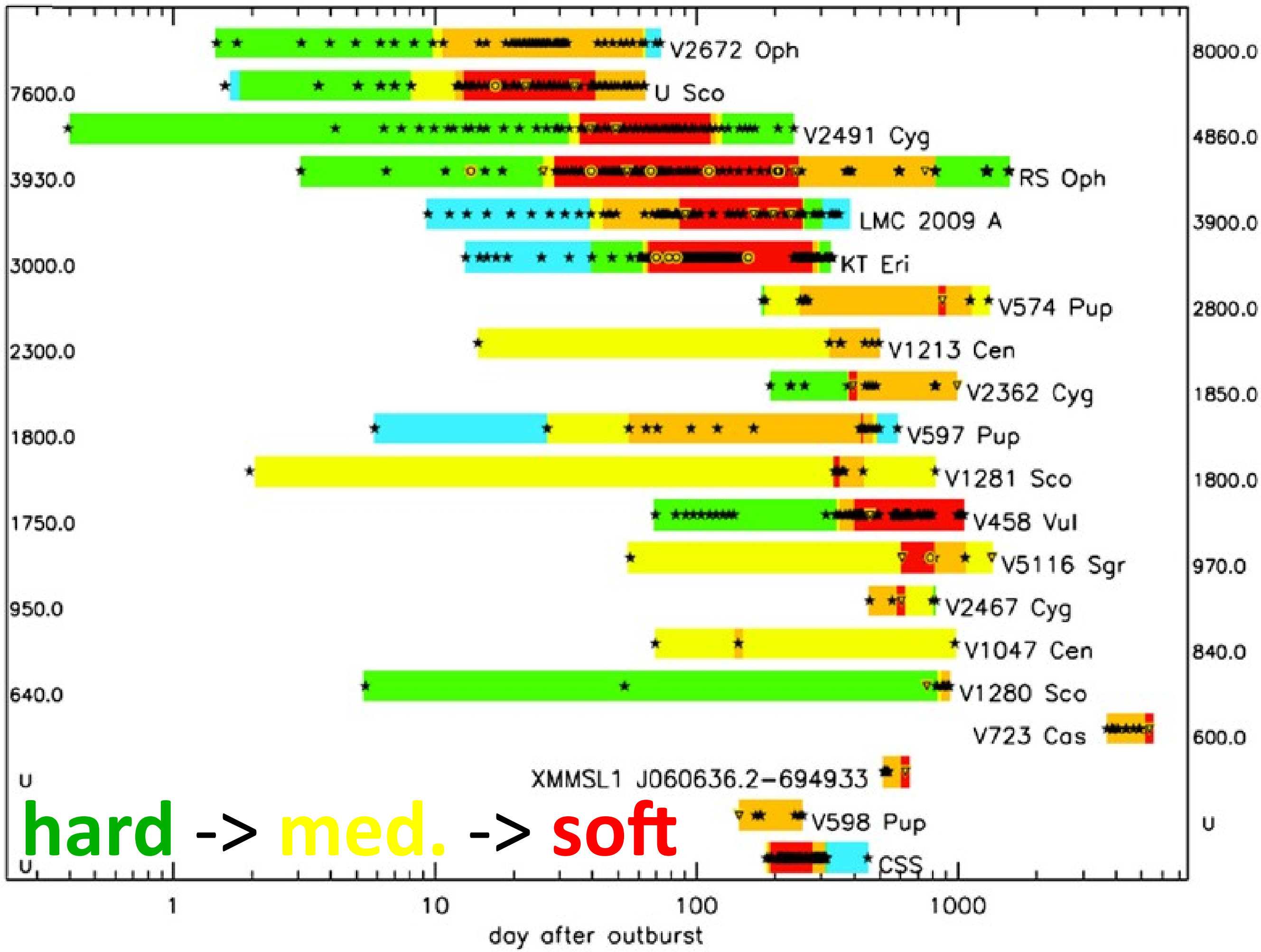

The pattern of X-ray emission in novae observed by Swift, ordered top to bottom by high to low optical emission line FWHM. Observations are shown by stars, intervals are colour coded by X-ray spectral state: blue = undetected; green = hard; yellow = intermediate; orange = most likely soft; red = soft. (From Schwarz et al., 2011).